Performance Enhancement of Vapor Compression Heat Pumps by a Cooled Compression Cycle

Arjomand Kermani, Nasrin; Terpollari Madsen, John ; Heerup, Christian; Elmegaard, Brian

Published in:
Proceedings of the13th IIR-Gustav Lorentzen Conference on Natural Refrigerants

Link to article, DOI:
10.18462/iir.gl.2018.1374

Publication date:
2018

Document Version
Peer reviewed version

DOI: 10.18462/iir.gl.2018.1374

PERFORMANCE ENHANCEMENT OF VAPOR COMPRESSION HEAT PUMPS BY A COOLED COMPRESSION CYCLE

Nasrin Arjomand Kermani[(a)], John Terpollari Madsen[(b)], Christian Heerup[(c)], Brian Elmegaard[(a)]

[(a)] Technical University of Denmark

Lyngby, 2800, Denmark, nasker@mek.dtu.dk, be@mek.dtu.dk

[(b)]Joma Tech,

Årslev, 5792, Denmark, Jm@surfpost.dk

[(c)]Danish Technological Institute,

Taastrup, 2630, Denmark, chp@teknologisk.dk

ABSTRACT

The presented study proposes a configuration combining the compression and condensation processes in a single unit and evaporation and expansion in another separate unit for application in a vapor compression heat pump cycle. The cycle includes injection of refrigerant into the compressor at a certain temperature. This system makes it possible to match the temperature glide of the heat sink and source and simultaneously condense the refrigerant during the compression.

A mathematical model of a complete cycle was made to study the system parameters and performance improvement of the cycle. Moreover, thermodynamic models of compression-condensation processes as well as a sensitivity analysis were developed to investigate the heat transfer inside the compressor-condenser unit and determine the injection conditions which can achieve the desirable requirements in the cycle model.
Advantages such as eliminating thermodynamic losses associated with the desuperheating of refrigerant, reduction of compression work, available hot liquid at the compressor outlet for the district heating system and COP closer to the Lorenz COP can be obtained compared to the conventional cycle. The proposed cycle reached COP of 4.1 and 59 % Lorenz efficiency for a case related to R717 as working fluid and district heating production.

Keywords: Heat pump, Combined compressor-condenser unit, refrigerant injection, Mathematical model, COP

1. INTRODUCTION

High efficiency and high performance heat pump systems are essential to provide energy efficient heat supply in domestic and industrial applications. Different approaches are followed with a view to improving system components, such as multi-stage compressors and expanders, and optimizing heat exchangers and complete systems. However, technologies such as multi-stage compressors and expanders can significantly affect the cost and complexity of these components. Hence, modifications to the basic cycle configuration can offer an alternative approach for providing better performance and increasing the competitiveness of these components in a broad range of applications. Two technologies, i.e., liquid-flooded compression processes and liquid/vapor-injection compression processes have been proposed as possible cycle modifications in which a remarkable performance improvement compared to conventional vapor compression cycle can be achieved.

The basic principle of liquid-flooded compression is adding a large amount of high specific heat fluid to the refrigerant flow at the inlet of the compressor. The extra fluid can absorb part of the energy added during the

compression process, consequently, reducing the discharge temperature of the refrigerant flow at the outlet of the compressor, and accordingly improve the performance of the whole cycle. An increase in cycle efficiency of about 5 % to 40 %, depending on the application, compared to a standard vapor compression system, when using an oil-flooded scroll compressor for a refrigeration system has been reported in (Bell et al., 2011). In addition, improvement of the coefficient of performance (COP) up to 13 % and 25 % for heating compared to the conventional vapor compression cycle has been reported in (Hugenroth et al., 2006) and (Ramaraj, 2013) for an oil-flooded scroll compressor respectively.

Alternatively, the liquid/vapor-injection compression is injecting refrigerant into the compressor to essentially reduce the discharge temperature, increase capacity, and finally enhance the performance of the cycle. Reducing the discharge temperature of the compressor using a liquid refrigerant-injected scroll compressor (Park et al., 2002), and reaching higher heating capacity of up to 30 % and higher COP of up to 20 % using a vapor-injection scroll compressor (Wang et al., 2009) have been reported previously. In addition, A COP improvement of nearly 9 % based on the same isentropic efficiency for the heat pump cycle combining the liquid-flooded and liquid-injection concepts has been reported by (Luo, 2016). The performance of vapor compression heat pumps using liquid-flooded and liquid-injection concepts have been compared by (Ramaraj et al., 2012) and concluded an improvement of COP for a vapor-injection cycle of up to 3 % and 13 % compared to a flooded compression cycle and the conventional vapor compression cycle. Moreover, considering an infinite number of injection ports (continuous injection) to maintain saturated vapor in the compressor can lead to significantly increase COP values of between 18 % and 51 % depending on the application (Mathison et al., 2011).

The present work proposes a heat pump cycle configuration combining compression and condensation in one single unit and evaporation and expansion in another separate unit while benefiting from the advantages of liquid refrigerant injection into both units at proper time with appropriate temperature glides matches with district heating system.

1.1 Cycle Configuration

A schematic view of the proposed vapor compression heat pump cycle is shown in Fig. 1. The specified evaporating temperature fixes the refrigerant properties as saturated vapor at the entrance of the compressor, point 1 in Fig. 1. The saturated vapor enters the compressor and is compressed adiabatically prior to injection into the compressor, point 2 in Fig. 1. For the rest of the compression processes, the liquid will be injected into the compression chamber to liquefy the superheated vapor into a saturated liquid with the required temperature and pressure at the outlet of the process, point 3 in Fig. 1. The liquid is injected at temperature and pressure which matches the temperature glide of the sink, i.e., a district heating system operating between 40 °C and 70 °C. This will provide the possibility of condensing refrigerant during the compression process while providing heat for the district heating system by subcooling the saturated liquid from point 3 to 4 in Fig. 1 and exchanging heat with the district heating system. After exiting the heat exchanger the sub-cooled liquid is split, into two streams, points 4 and 5 in Fig. 1. The former returns the subcooled liquid as compressor injection liquid, while the latter is the actual working fluid flow to the expansion. The subcooled liquid at point 5 in Fig. 1 expands adiabatically to point 6 in Fig. 1, before the heated expansion process from the lowest injection pressure to a two-phase mixture at the evaporating pressure, point 7 in Fig. 1. Similarly to the compressor-condenser unit, the expander and evaporator are also combined in a single unit in which the subcooled liquid will be expanded and evaporated simultaneously through injection to point 7 in Fig. 1. The two-phase mixture is split into points 8 and 1 in Fig. 1, which closes the cycle by returning the vapor phase to the compressor. The stream corresponds to point 8 in Fig. 1 directs the liquid phase of the refrigerant to the heat exchanger in which its pressure is increased, point 9 in Fig. 1, heated up by the heat source and returned back to the expander, point 10 in Fig. 1.

DOI: 10.18462/iir.gl.2018.1374

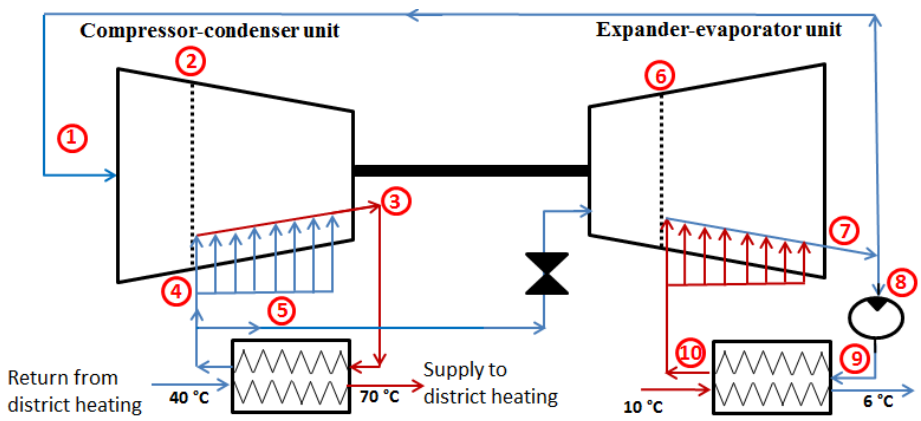

Figure 1. System configuration for the proposed vapor compression heat pump cycle

The paper is initiated by introducing, modeling and evaluating the performance of the proposed heat pump cycle compared to the conventional vapor compression cycle, and is completed by detailed dynamic analysis of the compressor-condenser unit that can fulfill the wanted conditions in the proposed cycle.

2. METHODS

2.1 Cycle Analysis

The performance of the proposed cycle was examined by numerical modeling of a cycle implemented in Engineering Equation Solver (EES) (Klein, 2017). The model was based on ammonia (R717) as refrigerant and first principles in terms of mass and energy balances for the all control volumes. The following assumptions have been used in the model which consists of 2536 equations which is solved in 4 seconds simulation time.

- A discretized positive displacement compression type with isentropic efficiency of 80 % and a volumetric efficiency of 100 %, of each segment
- Working fluid mass flow rate of 1 kg s^{-1}.
- The inlet and outlet of the heat sink and heat source were $T_{\text{sink-in}}, T_{\text{sink-out}}, T_{\text{source-in}}, T_{\text{source-out}}$ which were equal to 40 °C, 70 °C, 10 °C and 6 °C respectively.
- Temperature difference $\Delta T_{\min}$ equal to 2 K between the flows in the balanced heat exchangers.
- Pressure drop was neglected.
- Discretized expander with isentropic efficiency of 80 %, of each segment
- Pumping power was neglected

2.1.1 Compressor-condenser Model The compressor-condenser component was discretized equidistantly in temperature in up to 40 segments. The model assumed mixing to occur before compression. The mass balance and the energy balance equations, Eqs. (1) and (2) for the mixing were:

$$\dot{m}_{i+1} = \dot{m}_i + \dot{m}_{l,i} \qquad (1)$$

$$\dot{m}_{i+1} h_{m,i+1} = \dot{m}_i h_{i+1} + \dot{m}_{l,i} h_l \qquad (2)$$

where $\dot{m}_i$ is the mass flow rate of the refrigerant at the ith segment of the unit, $\dot{m}_{l,i}$ is the mass flow rate of the injected liquid into the ith segment of the compressor-condenser unit, and $h_{m,i+1}$ is the specific enthalpy of the refrigerant after mixing at the i+1th segment.
The compression power $\dot{W}_{\text{com}}$ was calculated based on the isentropic efficiency of the stage

$$\eta_{is,i} = \frac{h_{is,i+1} - h_{m,i}}{h_{i+1} - h_{m,i}} \qquad (3)$$

$$\dot{W}_i = \dot{m}_i\left(h_{i+1} - h_{m,i}\right) \text{ and } \dot{W}_{\text{com}} = \sum \dot{W}_i \quad (4)$$

where h_{is} is the specific enthalpy of the refrigerant assuming isentropic compression and $\dot{W}_{\text{com}}$ is the total compression power. Thermal equilibrium between the two phases was assumed both at the inlet, after liquid injection and at the outlet of each segment. Various mixing processes, such as linear enthalpy profile ($^{dh}/_{dp}$ = constant) and linear temperature profile ($^{dh}/_{dt}$ = constant), were evaluated. The former resulted in the lowest compression power and was selected for further analysis of the cycle performance. For the subcooling from point 3 to 4 in Fig. 1 the amount of heat transferred to increase the temperature from 40 °C to 70 °C for district heating application can be calculated from Eq. 5.

$$\dot{Q}_{\text{sink}} = \dot{m}_{l,\text{com-con}}(h_3 - h_4) \quad (5)$$

Where $\dot{m}_{l,\text{com-con}} = \sum \dot{m}_{l,i}$ is the total amount of liquid injected into the compressor-condenser unit.

2.1.2 Expander-evaporator Model Similar equations as for the adiabatic compression and cooled compression (Eqs. 1-4) were applied for adiabatic expansion and heated expansion to estimate the unknown parameters, for power produced, liquid injection and enthalpy. The amount of heat that transferred in the heat exchanger to increase its temperature from point 9 to 10 in Fig. 1 can be calculated from Eq. 6

$$\dot{Q}_{\text{source}} = \dot{m}_{l,\text{exp-evp}}(h_{10} - h_9) \quad (6)$$

Where $\dot{m}_{l,\text{exp-evp}} = \sum \dot{m}_{l,i}$ is the total amount of liquid injected into the evaporator-expander unit.

2.1.3 Cycle Performance The performance of the complete cycle was evaluated by combining the compressor-condenser unit with expander-evaporator model. The coefficients of performance of the cycle (**COP**) was calculated by

$$\text{COP} = \frac{\dot{Q}_{\text{sink}}}{\dot{W}_{\text{cycle}}} \text{ and } \dot{W}_{\text{cycle}} = \sum \dot{W}_{\text{com}} - \dot{W}_{\text{evp}} \quad (7)$$

Where $\dot{W}_{\text{cycle}}$ is the net power consumed. The COP was compared to the coefficients of performance for an ideal cycle, the Lorenz COP (COP_{lor}) given by the log mean temperatures between inlet and outlet of heat source and heat sink.

$$\text{COP}_{\text{lor}} = \frac{T_{\text{sink,lm}}}{T_{\text{source,lm}}} \; ; \; T_{\text{sink,lm}} = \frac{T_{\text{sink-in}} - T_{\text{sink-out}}}{\ln\left(\frac{T_{\text{sink-in}}}{T_{\text{sink-out}}}\right)} \text{ and } T_{\text{source,lm}} = \frac{T_{\text{source-in}} - T_{\text{ssource-out}}}{\ln\left(\frac{T_{\text{source-in}}}{T_{\text{source-out}}}\right)} \quad (8)$$

2.2 Dynamic Modeling of Compressor-condenser Unit

A thermodynamic model of a single-compression stroke of a reciprocating piston compressor was developed to investigate the heat transfer analysis inside the compressor-condenser unit and determine the injection conditions which can achieve the desirable requirements in the cycle model. The model was built based on the properties of ammonia (R717) using EES. It was based on assuming two separate control volumes inside the cylinder, transferring heat between each other. One control volume covered the refrigerant trapped inside the compression chamber, while the other covered the liquid refrigerant which was injected into the compression chamber during the process. The injected liquid was assumed to be sprayed into the cylinder as droplets. The compression chamber was a cylinder made of stainless steel (AISI 316). Inside diameter, and the stroke of the piston were 80 mm and 400 mm, respectively. Hence, the total displaced piston volume is 0.002 m^3. All conditions at inlet and outlet, and the properties of refrigerant at the injection moment were the same values as the ones assumed in the cycle model. Heat transfer to the environment through the walls was neglected based on (Arjomand Kermani and Rokni, 2015).

The thermodynamic model was based on first principles including the dynamic terms due to the change of mass and energy content during the compression. The model was used to investigate the development of

temperature of the two phases during the compression, e.g., to evaluate the assumption of thermal equilibrium.

2.2.1 Mass and Energy Balance The first control volume concerns the working fluid part of the refrigerant which is at constant mass. Since the compression will start after the inlet valve is closed, the energy conservation of the refrigerant trapped inside the compression chamber was determined from the first law of thermodynamics for a closed system as following:

$$\frac{dU}{dt} = \frac{\delta Q}{\delta t} - \frac{\delta W}{\delta t} \Leftrightarrow M\frac{\mathrm{du}}{dt} = \dot{Q} + P\frac{dV}{dt} \qquad (9)$$

where M is the total mass of vapor refrigerant entering the compression chamber at the beginning of the compression process, u is the specific internal energy of the refrigerant during compression, $\dot{Q}$ is the total rate of heat transfer between the refrigerant and injected liquid refrigerant, P is the pressure and V the volume, together determining the total compression power.

The mass and energy balances for an open system were employed for the liquid refrigerant injected into the compression chamber:

$$\frac{dM_{\mathrm{inj}}}{dt} = \sum \dot{m}_{\mathrm{inj}} \Leftrightarrow M_{\mathrm{inj}} = \int_{t_{\mathrm{inj}}}^{t} \dot{m}_{\mathrm{inj}}\, dt \quad (10)$$

$$\frac{dU_{\mathrm{inj}}}{dt} = \frac{\delta Q}{\delta t} - \frac{\delta W}{\delta t} + \frac{dH_{\mathrm{inj}}}{dt} \rightarrow \frac{d}{dt}(M_{\mathrm{inj}}u_{\mathrm{inj}}) = \dot{Q} - p\frac{dV}{dt} + \frac{d}{dt}\dot{m}_{\mathrm{inj}}h_{\mathrm{inj}} \qquad (11)$$

Where $\dot{m}_{\mathrm{inj}}$ is the mass flow rate of the injected liquid, which was assumed to be constant equal to be 8.2 kg s^{-1} (obtained in the cycle model). M_{inj} is the total mass of injected liquid refrigerant, and U_{inj} and H_{inj} are the internal energy and the enthalpy flow of the injected refrigerant entering the compression chamber at each time step, respectively. The rate of heat transfer between the refrigerant and injected liquid refrigerant was calculated based on (Qin and Loth, 2014)

$$\dot{Q} = nd\mathrm{Nu}K_{\mathrm{ref}}\pi(T_{\mathrm{ref}} - T_{\mathrm{inj}}) \quad (12)$$

Where n is the number of the liquid refrigerant droplets injected into the compression chamber, and d is their diameter. T_{inj} is the uniform temperature of injected liquid refrigerant at each time step during the compression procedure, K_{ref} and T_{ref} are the uniform thermal conductivity (for the gas phase) and temperature of refrigerant during the compression procedure and Nu is the Nusselt number calculated based on the Ranz-Marshall relationship (Barrow and Pope, 2007; Qin and Loth, 2014).

$$\mathrm{Nu} = 2 + 0.6\mathrm{Re}^{1/2}\mathrm{Pr}^{2/3} \quad \text{and} \quad \mathrm{Re} = \frac{\rho v D}{\mu} \qquad (13)$$

Where Pr is the Prandtl number calculated in EES based on temperature and pressure of the gas phase of the refrigerant inside the compression chamber and Re is the Reynolds number calculated based on uniform density (ρ) and viscosity (μ) of the gas phase of refrigerant inside the compression chamber, the diameter of the compression chamber (D), and (v) is the velocity of refrigerant determined by the initial volume flow rate of the refrigerant entered the compression chamber divided by the cross sectional area of compression chamber.

A sensitivity analysis was done to calculate appropriate $\dot{Q}$ values for fulfilling the wanted process from the cycle model, i.e., to determine the injection conditions such as number and diameter of liquid refrigerant droplets injected into the compression chamber based on Eqs. 12 and 13. The model was based on the assumption that the liquid injection was initiated at a compression pressure equal to saturation pressure at 42 °C and neglecting flash evaporation of the injected liquid refrigerant. The two control volumes were kept separate by neglecting the mixing of the condensed refrigerant with the injected refrigerant.

DOI: 10.18462/iir.gl.2018.1374

3. RESULTS

3.1 Cycle Performance

Fig. 2 shows the pressure-enthalpy (P-h) and temperature-entropy (T-S) diagram of the proposed cycle, the numbers shown in the red color corresponds to the points presented in Fig. 1.The performance of the proposed cycle is compared with the conventional vapor compression heat pump cycle (shown in green color).

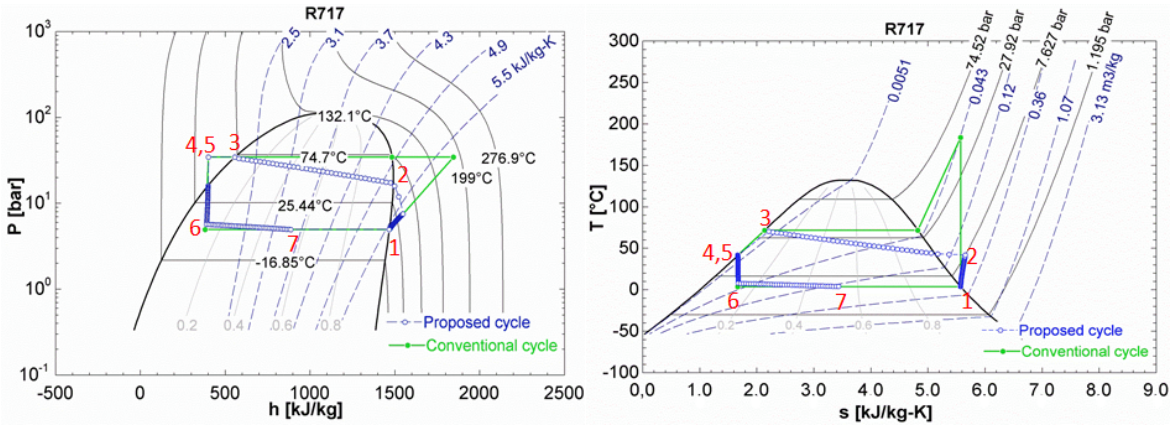

Figure 2. P-h and T-s diagram for the proposed cycle compared to conventional cycle for R717

As it can be seen from Fig. 2, injection of similar refrigerant at a proper condition can improve the performance of the cycle compared to the conventional vapor compression heat pump cycle. The total of 8.2 kg s^{-1} liquid refrigerant (in an increasing trend, starting from 0.1 kg s^{-1} at point 2 to 1.288 kg s^{-1} at point 3) and the total of 0.9 kg s^{-1} liquid refrigerant (in an increasing trend, starting from 0.01 kg s^{-1} at point 6 to 0.04 kg s^{-1} at point 7 was added to the compressor-condenser and expander-evaporator units, respectively. This amount of injected mass flow rate is relatively much greater than the suction mass flow rate. However, this can provide several advantages in every single component of the cycle compared to the conventional vapor compression heat pump cycle. For the compression process, as it can be seen from Fig. 2, advantages such as considerable reduction of discharge temperature ($T = 72$ °C at point (3), compared to $T = 184$ °C in the conventional cycle), lower temperature gradients inside the compressor, less operational problems with high temperature refrigerant and oil at the outlet of compressor. Furthermore, reduction of discharge temperature and eliminating the superheat region will provide advantages such as a large two-phase heat transfer region, consequently increasing the heat transfer coefficient and reducing temperature differences in the condenser. Similar advantages will be obtained in the expander-evaporator unit, and finally, reduction of the irreversibilities in each component of the cycle leads to better performance of the whole cycle.

The calculated COP for the presented cycle was equal to 4.1 with the ratio of $\mathrm{COP}/\mathrm{COP}_{\mathrm{lor}}$ equal to 0.59. The obtained values of COP was 4.03 for the conventional cycle. The improvement of COP (about 2 %) corresponds to a reduction of $\dot{W}_{\mathrm{cycle}}$ from 358 kW in the conventional cycle to 348 kW in the presented configuration, respectively.

The amount of COP improvement can change considerably depending on different parameters such as type of refrigerant (Mathison et al., 2011), and inlet and outlet temperatures of heat sink (Mathison et al., 2011) and heat source (Mathison et al., 2011; Ramaraj et al., 2012).
As an example, the COP improvement was 22 % for the inlet temperature of the sink of 30 °C and isentropic efficiency of 60 % in both the proposed cycle and conventional cycle. As explained above, the injection of liquid refrigerant will basically reduce the discharge temperature of the compressor; correspondingly reduce desuperheating losses in the condenser which explains the higher improvement in the cycle performance for lower inlet sink temperature and lower isentropic efficiency.

3.2 Dynamic Performance of Compressor-condenser Unit

Fig. 3 presents the results of the dynamic simulation for the compressor-condenser unit as well as the results obtained in the cycle model. The lines illustrated in the left side of P-h diagram, in the liquid region present

DOI: 10.18462/iir.gl.2018.1374

the changes in the properties of the liquid refrigerant injected into the compression chamber during the compression procedure for varying values of the heat transfer rate between the injected refrigerant and refrigerant inside the chamber. The red point in this region presents the properties of the injected liquid at the injection moment. On the other hand, the lines illustrated in the gas phase and two-phase regions in Fig. 3 present the changes in the properties of the refrigerant inside the compression chamber during the compression procedure, by increasing the heat transfer rate.

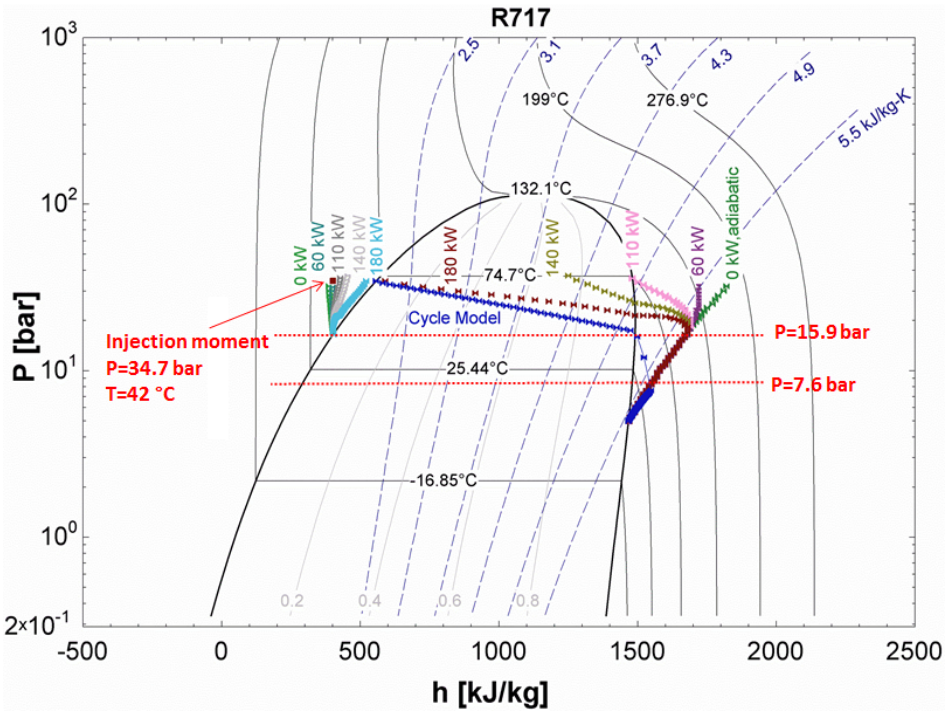

Figure 3. Enthalpy of R717 as function of pressure for different heat transfer rates between working fluid and the injected liquid during the compression procedure. The red point corresponds to the injection moment and the two red-dot lines correspond to the refrigerant pressure inside the chamber at the injection moment in the cycle and dynamic model

Fig. 3 shows that for high values of the heat transfer rate the enthalpy of the injected refrigerant increases at a certain pressure and gets closer to the liquid saturated line, while the enthalpy of refrigerant inside the compression chamber decreases. For a heat transfer rate equal to 180 kW, the enthalpy of the refrigerant inside the compression chamber starts decreasing immediately after the injection moment and reaches the results obtained in the cycle model at the end of compression processes, equal to a total of 0.0079 seconds.
Fig. 3 also illustrates that although the dynamic calculation is done based on similar cycle conditions as specified in Fig. 1, the injection moments occur later. This is mainly due to the simplified assumption of neglecting flash evaporation inside the compression chamber. Delaying the injection moment will generally increase the discharge temperature at point 2 in Fig. 1; corresponding to an increase in adiabatic compression work compared to the cycle model. This effect was neglected in the model.

Fig. 4(a-b) presents the changes in the pressure and temperature as a function of compression time assuming a heat transfer rate of 180 kW compared to adiabatic compression. Fig. 4(a-b) shows that the injection is started after 0.0047 s. From this moment the pressure and temperature corresponding to 180 kW heat transfer rate deviates significantly from the adiabatic case.

DOI: 10.18462/iir.gl.2018.1374

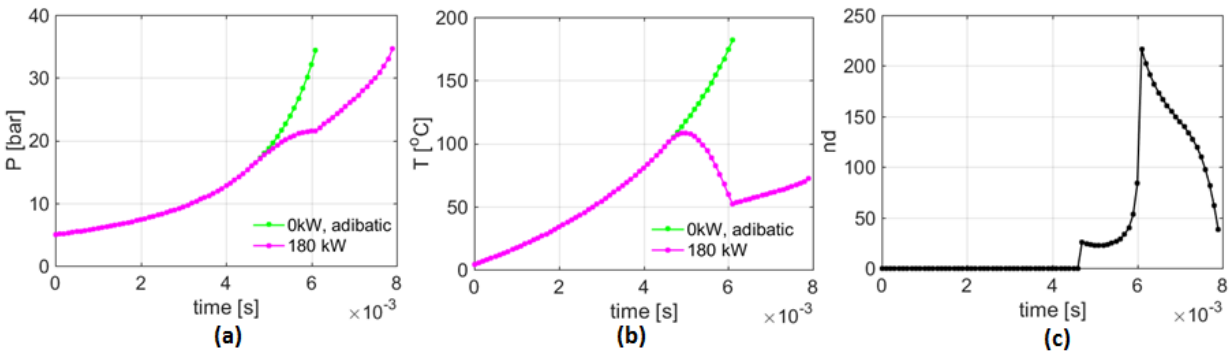

Figure 4. Changes of refrigerant (a) pressure, (b) temperature, and (c) number of droplets× diameter of droplets as a function compression time

Fig. 4-a shows that for the case of heat transfer rate equal to 180 kW at 0.0062 seconds – 0.0015 seconds after injection moment – there is a discontinuity in the increasing rate of pressure by time. This corresponds to the moment that the superheated refrigerant reaches the dew point. Furthermore, the corresponding significant reduction of refrigerant temperature at 0.0062 seconds can be seen in Fig. 4-b. This is mainly due to considerable heat transfer between the superheated refrigerant inside the compression chamber and the injected refrigerant; however this trend changes as soon as the superheated refrigerant enters the two-phase region. In the two-phase region, the temperature of the refrigerant slightly increases by increasing the compression time due to the increase in the pressure. Fig. 4-c shows the estimated values for nd (number of droplets × diameter of droplets) obtained from Eq.13. It can be seen that in agreement with the changes in pressure and temperature by time, nd also increases considerably 0.0015 seconds after the injection moment; however it gradually decreases as soon as reaching the two phase region.

3.3 R134a as working fluid

Fig. 5 presents the results obtained in the cycle and dynamic models for R134a by varying the heat transfer rate from 0 to 8.3 kW. The results obtained in the cycle model show that for R134a the average mass flow rate injected into the compressor-condenser unit to reach the condition presented in Fig. 1, is equal to 2.9 kg s^{-1}, compared to 8.2 kg s^{-1} for R717, for the same cylinder dimension and hence the suction volume flow rate. The heating capacity was in this case $\dot{Q}_{\text{sink}}$ 189.5 kW and $\dot{W}_{\text{cycle}}$ was 43 kW reaching a COP and Lorenz efficiency of 4.4 and 0.63, respectively. The cycle results are similar to the performance for R717, except for the lower capacity. For the dynamic model the process is considerably different from the results for R717. A higher tendency to enter the two-phase region is observed for the working fluid indicating the lower superheating of R134a and a relatively faster heat exchange between the phases.

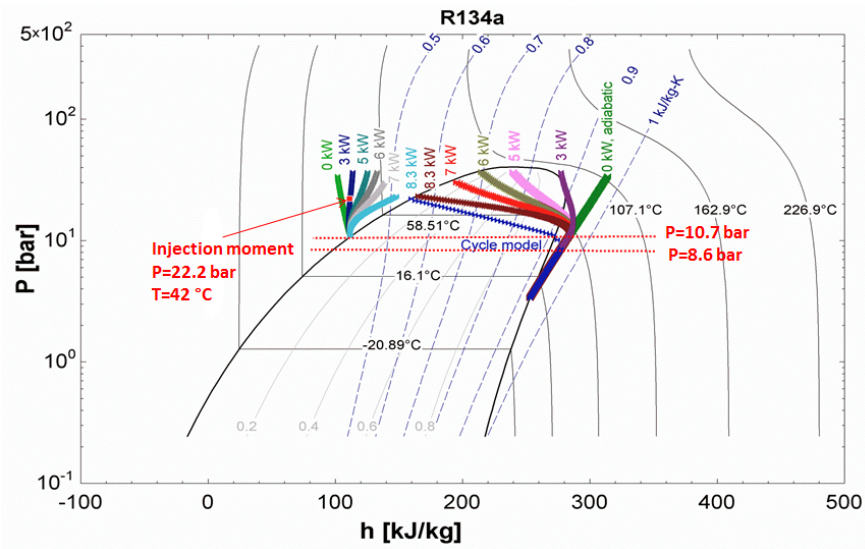

Figure 5. Enthalpy of R134a as function of pressure for different heat transfer rates between working fluid and the injected liquid during the compression procedure. The red point corresponds to the injection moment

and the two red-dot lines correspond to the refrigerant pressure inside the chamber at the injection moment in the cycle and dynamic model

4. DISCUSSION

The presented work proposed a new heat pump configuration and analyzed the potential performance enhancement that can be achieved compared to the conventional cycle. The performance enhancement depends on the choice of working fluid and the heat sink and heat source inlet and outlet temperatures thus the assumptions used in the model.

For the shown case of R717, the enhancement improvement is only about 2 % compared to the conventional cycle; however the performance can improve up to 20 % by reducing the inlet temperature of the sink to 30 °C and isentropic efficiency to 60 %. The shown cases are based on the assumptions such as constant isentropic efficiency as well as neglecting the pressure drops in the heat exchangers and irreversibilities due to the injection. Isentropic efficiency may vary depending on the type of compressor and the cycle conditions such as compressor inlet and outlet pressure (Lambers, 2008; Smith, 2005) . For the presented case, no definition for the isentropic efficiency of the compressor is available, and if the isentropic efficiency puts into relation to values which depend on the cycle performance, different results may obtain. In addition, pressure drop in the heat exchanger is neglected. However, it has been shown that increasing of the mas flow rate , which also happens in the proposed cycle due to the injection, can increase the pressure drop in the heat exchangers (Hsieh and Lin, 2003; Yan et al., 1999), consequently affect the cycle performance. Also, injection of the subcooled liquid into the superheated refrigerant correspondingly mixing procedure may cause irreversibilities (London, 1982) which in practice will reduce the obtained Lorenz efficiencies.

The dynamic model has identified the maximum amount of 180 kW and 8.3 kW heat transfer between the two phases for R717, and R134a respectively to achieve the desirable requirements in the cycle model. In practice, at the injection moment, flash evaporation may occur as the pressure of the injected liquid will suddenly drop to the equilibrium pressure inside the chamber (Sher et al., 2008). The effective heat transfer during flash evaporation can be desirable. However it can considerably affect the obtained results such as reducing the high heat transfer requirement between the two phases at the beginning of injection processes correspondingly smooth increasing of an injected mass flow rate instead of constant rate.
On the other hand, assumptions such as two separate control volumes between the injected liquid and working fluid inside the chamber, constant heat transfer rate between all the injected droplets and the working fluid from the injection moment up to the end of compression procedure, and finally gas velocity equal to piston velocity for calculating Re number, can affect the results. Depending on the relative velocity of the piston and droplets, as the piston getting closer to the top dead center, the droplets which have been injected at the earliest moments start sitting on the top side of the piston. Moreover, as the piston moves upward, the gas velocity might deviate from the piston velocity. Therefore estimating Re number based on swirl velocity might give us higher accuracy while leading to lower Re number (Arjomand Kermani and Rokni, 2015). Both cases will lead to reduction of the total heat transfer between the two phases, consequently increase the injection amount which might be difficult to reach or handle. Validation of the model by the experimental result can help in better understanding of the conditions that in practice may occur inside the chamber.

5. CONCLUSION

The present work proposes a heat pump cycle configuration combining compression and condensation in one single unit and evaporation and expansion in another separate unit while benefiting from the advantages of liquid refrigerant injection into both units at proper time to achieve temperature glide that matches the heat sink, e.g., a district heating system. The performance of the proposed cycle was examined by numerical modeling of the cycle and dynamic analysis of the compressor-condenser unit to point out the injection condition that can achieve the conditions suggested by the cycle model. The proposed cycle reached COP of 4.1 and 59 % Lorenz efficiency for a case related to R717 as working fluid and district heating production.

The obtained results show that compared to the conventional vapor compression heat pump cycle, the presented configuration has potential for improving the performance of heat pumps. The parametric studies show that the performance improvement of the cycle depends on different parameters such as type of refrigerant, heat sink and heat source temperature and isentropic efficiency. The model can be used for further optimization purposes to identify the applications that can provide the most potential for improved performance.

ACKNOWLEDGEMENTS

The work was funded by the Elforsk Program; Project number 349-040 Cooling plant using temperature glide.

NOMENCLATURE

Abbreviation

COP	Coefficient of performance	EES	Engineering Equation Solver

Symbols

D	chamber diameter (m)	$\dot{Q}$	heat flow rate (kW)
d	droplet diameter (m)	Re	Reynolds number (-)
h	specific enthalpy ($kJ \cdot kg^{-1}$)	s	specific entropy ($kJ \cdot kg^{-1} \cdot K^{-1}$)
K	thermal conductivity ($W \cdot m^{-1} \cdot K^{-1}$)	T	temperature (°C)
M	mass (kg)	t	time (s)
$\dot{m}$	mass flow rate ($kg \cdot s^{-1}$)	u	specific internal energy ()
Nu	Nusselt number (-)	V	chamber volume (m^3)
n	number of droplets (-)	v	velocity ($m \cdot s^{-1}$)
P	pressure (bar)	$\dot{W}$	work rate (kW)
Pr	Prandtl number (-)		

Greek letters

μ	dynamic viscosity (Pa·s)	η	efficiency
ρ	density ($kg \cdot m^{-3}$)	Δ	difference

Sub-&super scripts

com	compressor	inj	injection
con	condenser	is	isentropic
evp	evaporator	m	mixing
exp	expander	l	injected liquid refrigerant
i	i^{th} segment	ref	refrigerant

REFERENCES

Arjomand Kermani, N., Rokni, M., 2015. Heat transfer analysis of liquid piston compressor for hydrogen applications. Int. J. Hydrogen Energy 40, 11522–11529.

Barrow, H., Pope, C.W., 2007. Droplet evaporation with reference to the effectiveness of water-mist cooling. Appl. Energy 84, 404–412.

Bell, I.H., Groll, E.A., Braun, J.E., 2011. Performance of vapor compression systems with compressor oil flooding and regeneration. Int. J. Refrig. 34, 225–233.

Hsieh, Y.Y., Lin, T.-F., 2003. Evaporation Heat Transfer and Pressure Drop of Refrigerant R410a Flow in a Vertical Plate Heat Exchanger. J. Heat Transfer 125, 852–857.

Hugenroth, J., Braun, J., Groll, E., King, G., 2006. Oil flooded compression in vapor compression heat pump systems, in: IHR-IRHACE Conference. pp. 492–9.

Klein, S., 2017. Engineering equation solver academic professional v10.273-3d.

Lambers, K.J., 2008. Isentropic and Volumetric Efficiencies for Compressors with Economizer Port, in: International Compressor Engineering Conference. p. 9.
London, A.L., 1982. Economics and the second law: An engineering view and methodology. Int. J. Heat Mass Transf. 25, 743–751.
Luo, B., 2016. Oil flooded compression cycle enhancement for two-stage heat pump in cold climate region: System design and theoretical analysis. Energy Convers. Manag. 115, 52–59.
Mathison, M.M., Braun, J.E., Groll, E.A., 2011. Performance limit for economized cycles with continuous refrigerant injection. Int. J. Refrig. 34, 234–242.
Park, Y.C., Kim, Y., Cho, H., 2002. Thermodynamic analysis on the performance of a variable speed scroll compressor with refrigerant injection. Int. J. Refrig. 25, 1072–1082.
Qin, C., Loth, E., 2014. Liquid piston compression efficiency with droplet heat transfer. Appl. Energy 114, 539–550.
Ramaraj, S., 2013. Vapor Compression Cycle Enhancements for Cold Climate Heat Pumps. Master Thesis 82.
Ramaraj, S., Song, Y., Braun, J.E., Horton, W.T., 2012. Vapor Compression Cycle Enhancements through Liquid Flooded Compression with Regeneration and Dual-Port Refrigerant Injection, in: Seventh International Cold Climate HVAC Conference. Calgary, Canada, pp. 240–247.
Sher, E., Bar-Kohany, T., Rashkovan, A., 2008. Flash-boiling atomization. Prog. Energy Combust. Sci. 34, 417–439.
Smith, R., 2005. Chemical process design and integration. John-Wiley.
Wang, X., Hwang, Y., Radermacher, R., 2009. Two-stage heat pump system with vapor-injected scroll compressor using R410A as a refrigerant. Int. J. Refrig. 32, 1442–1451.
Yan, Y.-Y., Lio, H.-C., Lin, T.-F., 1999. Condensation heat transfer and pressure drop of refrigerant R-134a in a plate heat exchanger. Int. J. Heat Mass Transf. 42, 993–1006.